DOI: 10.1021/ma1005028

Macromolecules
ARTICLE

Electromechanical Properties of Smectic C* Liquid Crystal Elastomers under Shear

Periklis Papadopoulos,*,† Patrick Heinze,‡ Heino Finkelmann,‡ and Friedrich Kremer†

†*Institute for Experimental Physics I, Fakultät für Physik und Geowissenschaften, Universität Leipzig, Linnéstrasse 5, 04103 Leipzig, Germany, and* ‡*Institute for Macromolecular Chemistry, Albert-Ludwigs-Universität Freiburg, Freiburg im Breisgau, Germany*

Received March 5, 2010; Revised Manuscript Received May 20, 2010

ABSTRACT: Liquid crystal elastomers combine the electrical and optical properties of liquid crystals with the mechanical ones of polymer networks. In smectic C systems, doping with chiral mesogens induces the formation of domains with permanent electric dipole moment, which exhibit piezoelectric properties. Orientation of the mesogen in a uniaxial mechanical field and subsequent cross-linking produce a centrosymmetric morphology, where the piezoelectric effects are averaged out on a macroscopic length scale. The application of shear breaks the symmetry and induces the formation of a monodomain structure. In this study the measurements of the direct piezoelectric effect are compared with the recently published structural changes during stepwise shear. It is shown that the piezoelectric coefficient reaches its maximum at a certain shear angle that corresponds to the intrinsic smectic tilt angle. The complex electromechanical coefficient may vary up to a factor of 2 in a broad temperature, static mechanical stress and frequency range. The response of the system remains linear, the higher harmonics contributing no more than ∼10% in any case.

Introduction

Liquid crystalline elastomers (LCEs) have attracted interest in the last years, because they combine the orientational properties of liquid crystals with the elasticity of conventional cross-linked polymer networks (elastomers). The network prevents the system from flowing in any directions, unlike low molecular weight liquid crystals. As a result, they exhibit electro-mechanical and electro-optical properties that can potentially surpass the ones of conventional systems. The ease of processing makes them candidates for several applications, such as flexible displays, electromechanical actuators, and artificial muscles.[1]

In general, several types of LCEs can be distinguished, depending on the liquid crystalline phase and the position of the mesogen with respect to the network. Both side- and main-chain LCEs with either nematic or smectic order have been synthesized.[2−7] In main-chain systems, where the mesogen is part of the polymer network, the orientation of the director is strongly coupled to the macroscopic network orientation.

Chiral smectic C* systems have no point symmetry and can exhibit a macroscopic permanent dipole moment.[8−11] Their piezoelectricity is a direct consequence of ferroelectricity and is related to the electroclinic effect.[4,12−14] The origin of the dipole moment and its orientation with respect to the director has been discussed in previous works.[12] Soft, but nonflowing piezoelectric films can be manufactured by incorporation into a polymer network. The electromechanical properties of cholesteric and SmC* LCE systems have been previously investigated. Both the direct[12,15,16] and inverse[17,18] piezoelectric effects in ferroelectric LCE as well as the electroclinic effects[13,14,19] have been studied as a function of temperature, sample orientation, dc-bias and mechanical strain.[20] The reorientation of the mesogen due to the applied electric field, especially in thin films, gives rise to electrostriction and second harmonic generation.[21]

*Corresponding author. E-mail: papadopoulos@physik.uni-leipzig.de.

A challenge in the chiral systems is the formation of monodomain morphology; otherwise the electro-mechanical effects are averaged out.[4,22] Ideally, a liquid single crystal elastomer (LSCE) should be used. The synthesis of SmC* leads to the formation of a chevron microstructure.[23] The mesogens can be oriented using magnetic, electric or mechanical fields.[24−27] The magnetic fields, however, can only orient the director, due the diamagnetism of the aromatic rings, without largely affecting the smectic layers. On the other hand, electric fields could create monodomain samples,[13] but the saturation fields are of the order of 10^7 V/m, which cannot be safely applied to films thicker than a few μm. The remaining possibility is the application of (biaxial) shear mechanical fields.[25,28,29]

In a recent X-ray study the conversion of a pseudomonodomain structure, with a uniform director orientation, but conical distribution of layer normals, to liquid single crystal morphology in a series of SmC*-LCE under shear has been reported.[30] The shear was applied perpendicular to the director.[29] It was found that shear gradually aligns macroscopically the smectic layers and the order parameter of the director reaches a maximum at an angle ∼30°. However, the formation of liquid single crystal remains incomplete, even at high shear angles. In this study we attempt to find the optimal processing conditions for ferroelectric LCE, by measuring the direct piezoelectric effect as a function of shear in one of these LCE systems. It is found that the piezoelectric coefficient is initially zero, but reaches a maximum at the shear angle, where the highest director order parameter is observed. In addition, a complete temperature and frequency dependence of the piezoelectric coefficient is presented.

Experimental Section

A schematic of the microstructure of the SmC* elastomer is shown in Figure 1. The content of chiral dopant is 7.3 wt %. Its synthesis and calorimetric properties have been reported recently.[30] It exhibits a broad SmC* temperature range, with an

 Published on Web 07/28/2010

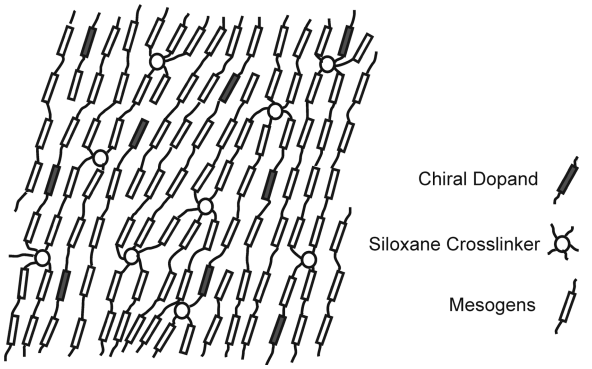

Figure 1. Structure of the main-chain SmC* elastomer. A chiral dopant is added to 7.3 wt % in order to induce the formation of domains with permanent electric dipole moment, making the elastomer ferroelectric.

isotropization temperature of 69 °C. Below 5 °C a tilted hexagonal smectic phase is formed and the glass "transition" is observed at −2 °C. The thickness of the sample is ∼350 μm. The custom-made measurement cell allows the measurement of the piezoelectric coefficient d_{33} using the direct piezoelectric effect, under well-controlled temperature conditions.[12,21,31,32] The details of the setup are shown in Figure 2. The shear angle β is increased stepwise using the device of Figure 2a and can reach 45° in steps of 2°. The electrodes that are attached to each side of the sample are so designed, that they apply uniform mechanical pressure, while measuring the generated charge over a small area. This area should be kept as small as possible, otherwise the effects are averaged out, before the conversion of the polydomain morphology to a monodomain one. The size of domains with uniform layer orientation is not well-known, but electrodes with size around 1 mm^2 give better reproducibility than larger ones. The plastic boards are d_F = 5 mm wide and have an d_e = 1 mm wide copper stripe, resulting in a conductive overlapping area of ∼1 mm^2. The large ratio of the area where force is applied to the conductive area ensures that a uniform mechanical field is applied to the latter, avoiding artifacts due to pressure inhomogeneity and local shear at the edges. The thickness of the sample is large enough to ensure that the mechanical stress remains uniform even with the inevitable small electrode misalignment. The shearing part with the sample and electrodes are finally placed between a piezocrystal that controls the sample's deformation and a force transducer (Burster GmbH) that measures the applied force with high time resolution (down to 0.5 ms using the digital output). Unless otherwise specified, sample deformation is lower than 5% to ensure a linear response. The whole setup is kept in a cryostat and is removed only for a few seconds when shear is increased. The measurements are carried out at ∼50 °C in order to ensure that the sample is in the smectic C phase. The X-ray measurements were also performed at 50 °C.[30]

The pressure-generated surface charge leads to current flow. Using lock-in amplifiers (Stanford Research Systems SR 830) the phase differences between the applied strain and generated charge as well as mechanical stress can be resolved. The sample electrodes are connected directly to the input of a lock-in amplifier. In order to minimize parasitic currents a resistor of 1 MΩ is connected parallel to them resulting to a total complex input impedance of Z = 950 kΩ // 150 pF, including connecting cables. The coefficient d_{33} can be related to the measured voltage V and force F through

$$V = Z\frac{\mathrm{d}q}{\mathrm{d}t} = ZA_e d_{33}\frac{\mathrm{d}P}{\mathrm{d}t} = Z\frac{A_e}{A_f}d_{33}\frac{\mathrm{d}F}{\mathrm{d}t} \qquad (1)$$

where A_e is the conductive area of the electrodes, A_f the total (overlapping) area of the plastic boards, P the applied stress, and F the applied force. When sinusoidal strain is applied, one gets,

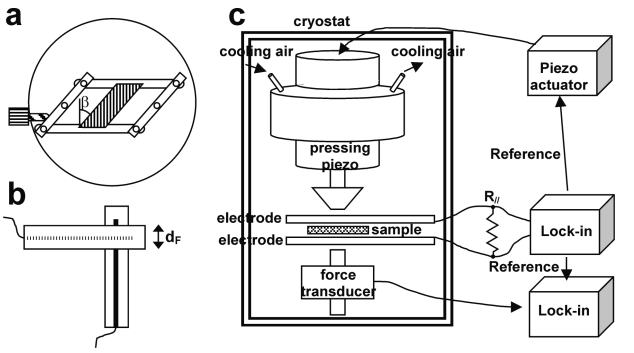

Figure 2. Measurement of the direct piezoelectric effect on the SmC* elastomer. (a) The shearing part (viewed from above) allows shearing the sample up to β = 45° in steps of 2° using a screw. (b) The electrodes are designed so that the effects are not averaged out due to the centrosymmetric morphology. The total conductive area is d_e^2 = 1 mm^2, whereas the overlapping area of the plastic boards is d_F^2 = 25 mm^2. (c) The shearing part, the piezo crystal and the force transducer are in a cryostat whose temperature is controlled by nitrogen gas. The electrodes and the output of the force transducer are connected to lock-in amplifiers, one of which controls the piezo actuator. The amplitudes of the generated voltage and force, as well as their phase shifts with respect to strain, can be acquired with high accuracy.

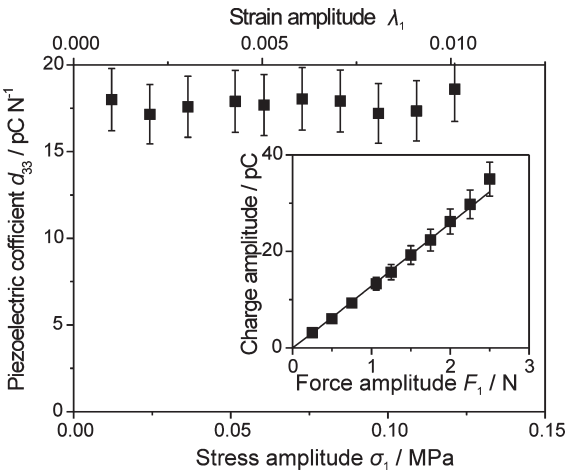

Figure 3. Direct piezoelectric effect. A sinusoidal mechanical field at f = 100 Hz is applied to a sample that has been sheared at β = 22° and the generated ac voltage is measured. From their ratio the piezoelectric coefficient can be calculated. The static mechanical stress is 0.15 MPa. Nonlinearity effects are not observed up to this value of static mechanical stress.

using complex values for sinusoidally varying quantities and assuming linear response

$$d_{33} = -i\frac{A_f V}{A_e Z\omega F} = \frac{A_f V_1}{A_e|Z|\omega F_1}\exp(i(\varphi_V - \varphi_f - \delta)) \qquad (2)$$

where V_1 and F_1 are the amplitudes of the voltage and force, φ_V and φ_f the respective phases, and δ the loss angle of the input impedance. The lock-in amplifiers allow the measurement of the second harmonic of both charge and force, as well. The respective equations, where the second harmonic is also included, are shown in detail in the Supporting Information and have been applied in the case of high sample deformation only. At low sample deformations the sample shows a strictly linear response.

An application example is shown in Figure 3. The sample is already sheared; otherwise the piezoelectric coefficient is nearly zero. The generated charge and, hence, the voltage are proportional to the applied force, or mechanical stress. The quantities that will be used below are the piezoelectric coefficient and the

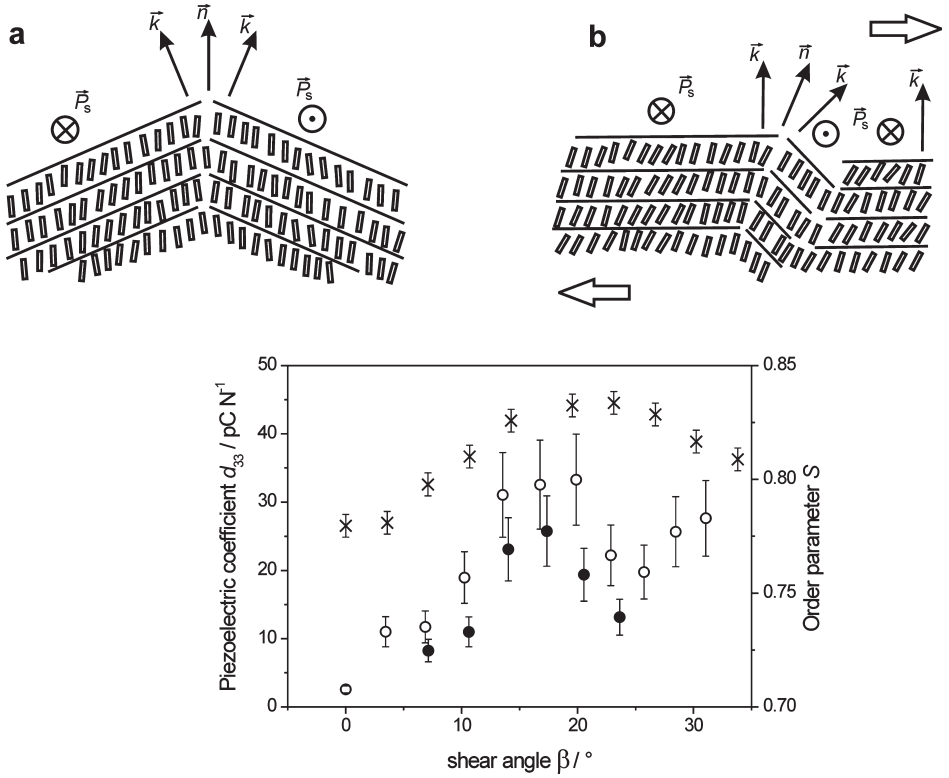

Figure 4. Effects of shear. (a) The director $\vec{n}$ is initially oriented, but the LCE exhibits a centrosymmetric morphology with conical distribution of layer normals $\vec{k}$. The direction of the spontaneous polarization $\vec{P}_S$ in each domain is normal to both $\vec{n}$ and $\vec{k}$. (b) After shearing a pseudomonodomain structure is obtained, with an almost uniform smectic layer normal and polarization orientation. Only 10% (suggested by X-rays) retain the opposite polarity. (c) The conversion to pseudomonodomain structure is reflected on the increase of the piezoelectric coefficient. In both independent measurements (circles, two different samples) a clear maximum around 15−20° is observed, coinciding with the maximum director order parameter (crosses).[30] The measurements are carried out at f = 100 Hz, 0.004 strain amplitude, under a static stress of 0.05 MPa (static strain of ~0.005).

mechanical stress, which do not depend on the geometry of the sample and the experimental setup. The results are stable in this stress and temperature range at least for a few days.

Results and Discussion

The aim of this investigation is the detailed measurement of the dependence of d_{33} as a function of sample shear. In a previous report, the reorientation of the LCE sample upon shear deformation was investigated by X-ray diffraction.[30] To allow comparison to our results, a sample of the same composition and the same shear geometry and experimental conditions as in the X-ray study is used.

The main-chain mesogens in the LCE under study possess an electric dipole moment with a component normal to the director. The macroscopic spontaneous dipole moment is proportional to the angle θ formed by the director $\vec{n}$ and the smectic layer normal $\vec{k}$ (Figure 4a). Therefore, the tilted chiral smectic phase exhibits a spontaneous macroscopic dipole moment along the C_2 symmetry axis (z-axis in this case) and is ferroelectric. Polarization density and sample dimensions are, thus, closely interrelated through the angle θ, giving rise to the electroclinic effect.[12] The existence of domains with different orientation of the smectic layers and, hence, polarity averages out the electromechanical effects. The goal of this work is to find the optimal processing conditions leading to a high macroscopic orientation of the dipoles and, hence, high polarization. The first necessary condition is the orientation of the director, which is done during cross-linking. However, even though the director is oriented, the spontaneous polarization vectors are conically distributed. When the sample is sheared, the smactic layers start to align along shear direction. Even though polydomain morphology still exists, the total polarization density is no more equal to zero and, thus, ferroelectricity can be observed on macroscopic scale (Figure 4b). The dependence of the piezoelectric coefficient as a function of shear angle is presented in Figure 4c. As expected, before the application of shear, the measured piezoelectric coefficient is nearly zero. The polarity of the generated charge depends on the shear direction; using the geometry of Figure 2a and 4b, a negative charge is generated at the front surface, when the sample is pressed.

As the sample is sheared the piezoelectric coefficient rises and reaches a maximum at ~20° shear angle, close to the angle where the highest director order parameter is observed with X-rays.[30] The director order parameter is defined as the product $S = S_n S_d$, where S_n is the nematic and S_d the domain order parameter, both defined by the second-degree Legendre polynomial. Further shear leads to a decrease of the coefficient. This effect seems to be related to breakup of the sample structure into domains, resulting to the decrease of the director order parameter. A real monodomain structure is, therefore, not obtained. Theoretical studies have shown that the director in half of the domains has to move along a long path, before being aligned.[25] It is possible that the layers are rotated so that the static polarization $\vec{P}_S$ is no more exactly normal to the sample surface and the electrodes, decreasing the average charge, when pressure is applied.

The application of LSCE as electromechanical actuators requires detailed knowledge about the influence of external conditions on the piezoelectric coefficient. The samples used for this series of measurements are prepared by shearing the sample at 22°, where the piezoelectric coefficient is maximum. The frequency dependence is shown in Figure 5. A clear decreasing trend with increasing frequency is observed (Figure 5a), despite

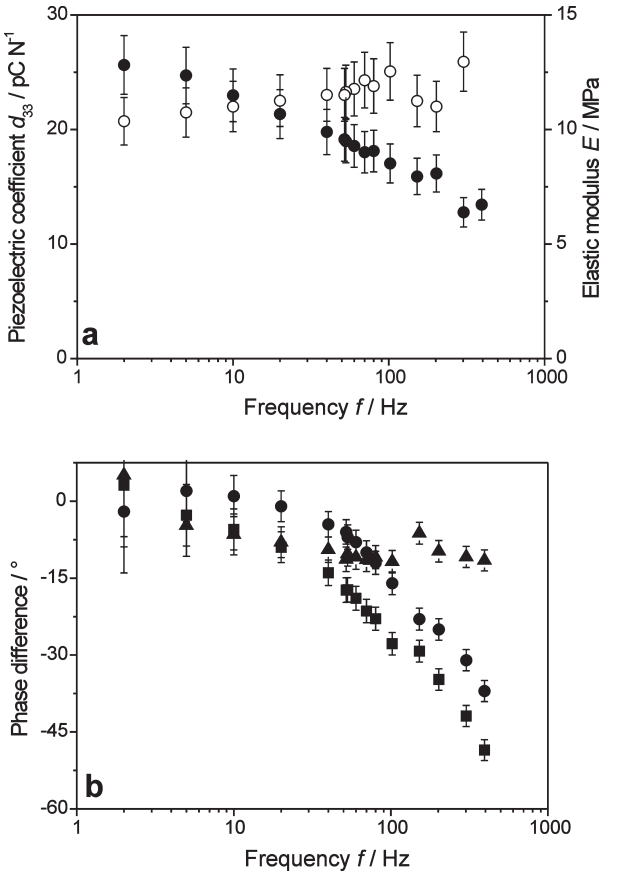

Figure 5. Dependence of electromechanical properties on frequency. (a) The absolute value of the complex piezoelectric coefficient d_{33} (solid symbols) drops by a factor of 2 from its static value up to 400 Hz. The respective elastic modulus E (open symbols) has a weakly increasing trend with frequency. (b) Phase differences between charge and strain ($\varphi_V - \delta$, squares), stress and strain (φ_f, circles) and charge and stress ($\varphi_V - \varphi_f - \delta$, triangles). The latter is almost zero and varies only weakly with frequency and no resonance is observed. All measurements are carried out using strain amplitude 0.004, shear angle $\beta = 22°$, static stress $P_0 = 0.06$ MPa.

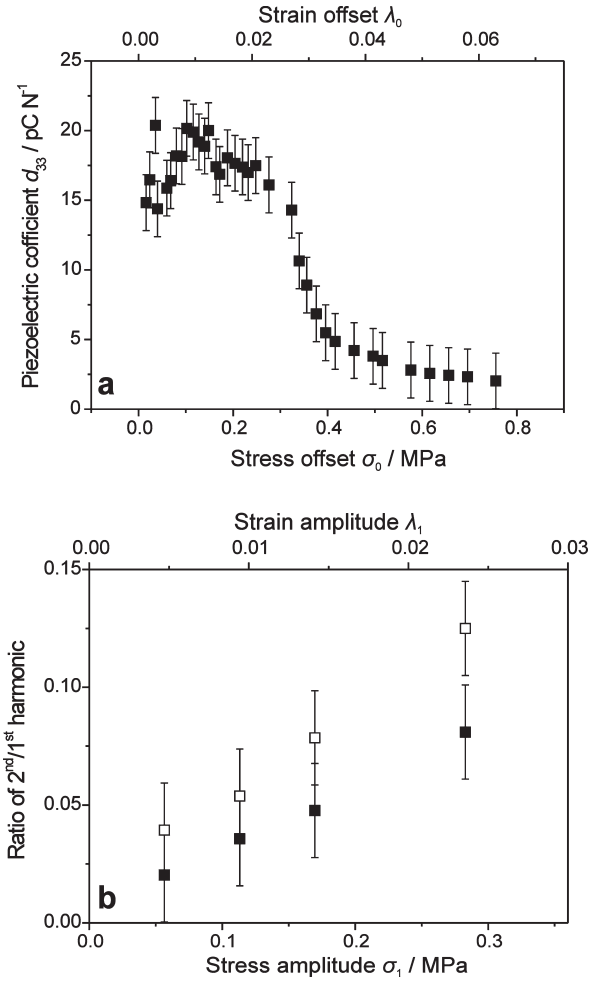

Figure 6. Nonlinearity of the direct piezoelectric effect. (a) Dependence of the piezoelectric coefficient on static stress. The strain amplitude is 0.004, $\beta = 22°$, $f = 100$ Hz. A strong decrease is observed, when static stress P_0 exceeds ~0.3 MPa. (b) The ratio of the amplitudes of the second and first harmonics of force (solid symbols) and charge (hollow symbols) is quite low up to stress amplitudes of 0.3 MPa. The same trend is observed for shear angles β in the range 18−32° (not shown).

the almost constant absolute value of the elastic modulus over the three decades of frequency (Figure 5b). This result is not related to the resonance of the system; the resonance frequency calculated by

$$f_R = \sqrt{E/\rho}/2h \quad (3)$$

for a free-standing film,[33] where E is the elastic modulus, h the thickness of the sample, and ρ the density, gives a value of ~140 kHz, well above the measurement range. The mechanical loss angle $|\varphi_f|$, however, increases dramatically above 10 Hz and shows that the large dissipation of mechanical energy at high frequencies is responsible for the decrease of the measured piezoelectric coefficient. It is remarkable that the phase angle between stress and charge $\varphi_V - \varphi_f - \delta$ has an almost frequency-independent low value $< 10°$, due to the strong coupling between the network and the smectic microstructure in main-chain LCE.[22]

The piezoelectric actuator should also maintain its properties under external stress. The (dynamic) piezoelectric coefficient as a function of static mechanical stress is shown in Figure 6. It is constant up to stress of ~0.3 MPa, corresponding to a static deformation of about 3%, but then decreases dramatically approaching zero. The second harmonic generation in LSCE due to electrostriction effects has been shown to affect significantly the electromechanical properties of such systems.[12,21] However, in this system the second harmonic of both the generated stress and charge remain lower by about 1 order of magnitude than the first harmonic (Figure 6b). The decrease of the electromechanical response is, therefore, attributed to the distortion of the monodomain morphology due to the large (more than 5%) static sample deformation. On the other hand, the application of large deformation at higher frequencies does not affect the morphology, probably due to the long sample relaxation times. Compared to inorganic piezocrystals, the soft LCE actuators can bear much larger strain.

Finally, the observed temperature dependence is quite unusual for chiral smectic LCE exhibiting phase transitions[34] and is more similar to inorganic systems. The peak of the piezoelectric coefficient in the first heating run (Figure 7a) just before the smectic to isotropic transition is followed by a sharp irreversible decrease to zero. Since the director distribution becomes isotropic, cooling the sample below T_{SI} does not induce spontaneous polarization, without reorienting the sample using mechanical fields. The DSC and X-ray results[30] are in good agreement with the observed transition temperature of 71 °C. In contrast to previous studies[34] no resonance is observed, the phase difference between strain and charge showing only weak temperature dependence (Figure 7b). This result shows that the network relaxation times in this temperature range are much shorter than

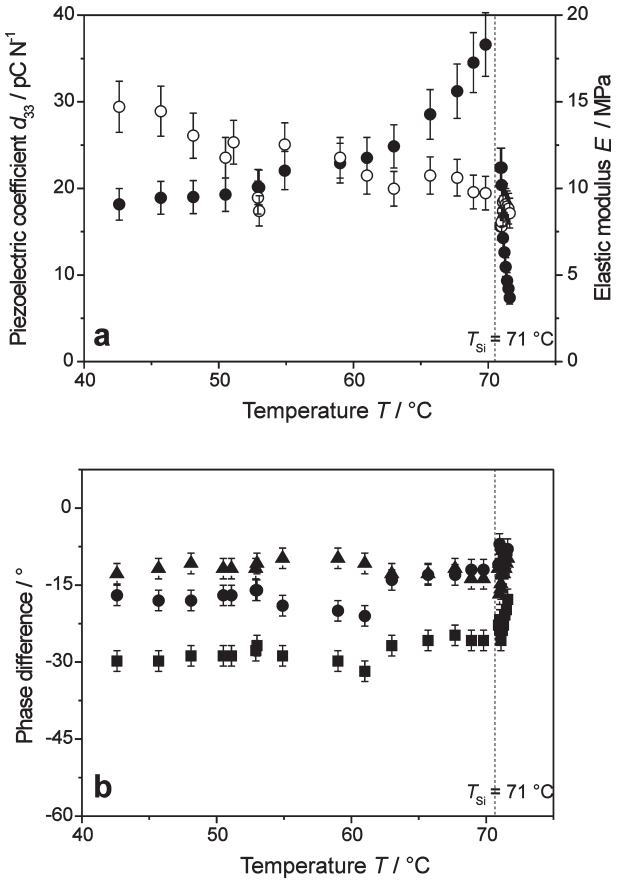

Figure 7. Temperature dependence of the electromechanical effects. (a) The piezoelectric coefficient d_{33} (solid symbols) in the first heating run increases until the SmC* to isotropic transition temperature T_{SI}. A sharp irreversible drop is observed afterward. The elastic modulus E (open symbols), on the other hand, shows a decreasing trend, with only a small step at T_{SI}. (b) The phase differences between charge and strain ($\varphi_V - \delta$, squares), stress and strain (φ_f, circles) and charge and stress ($\varphi_V - \varphi_f - \delta$, triangles) are weakly affected by temperature. The strain amplitude is 0.004, shear angle $\beta = 22°$, $f = 100$ Hz. The static stress is $P_0 \sim 0.10$ MPa, corresponding to a static strain of $\sim$0.01.

the time-scale of the experiment (10 ms), in agreement with DSC that gives a T_g value around -2 °C.

Conclusions

The electromechanical properties of a SmC* LCE have been characterized as a function of shear, external stress, frequency and temperature. The study shows that shear processing is an effective way to produce electromechanically active liquid crystal eleastomers from uniaxially oriented films. The exact shearing parameters are crucial for the production of optimal samples. Incomplete conversion of the polydomain to monodomain morphology leads to the averaging out of the observed effects in large samples. The maximum piezoelectric coefficient d_{33} is observed at shear angles of 18°. At this shear angle, the smectic layers and thus the dipole vectors still undergo realignment and thus at higher shears higher values of the permanent polarization are measured. On the other hand, the X-ray studies revealed that at slightly higher shear angles the system breaks up into domains of two independent director orientations. The piezoelectric coefficient therefore seems to be dependent on both the smectic layer structure and the director order parameter.

The response of the system to external pressure remains practically linear up to strain of 3% and stress of 0.3 MPa, so the contribution of higher harmonic remains below $\sim$10% in all investigated cases. The piezoelectric coefficient does not change by more than a factor of 2 within a broad frequency, temperature and static deformation range. In addition, the loss angle (between stress and generated charge) maintains an almost constant low value. For these reasons, this SmC* LCE can be used as a soft electromechanical actuator for frequencies below the kHz range, at temperatures ranging from the glass transition up to the smectic to isotropic transition.

Supporting Information Available: Text giving the derivation of nonlinear term of the piezoelectric coefficient. This material is available free of charge via the Internet at http://pubs.acs.org.

References and Notes

(1) de Gennes, P. G.; Hébert, M.; Kant, R. *Macromol. Symp.* **1997**, *113*, 39.
(2) Greve, A.; Finkelmann, H. *Macromol. Chem. Phys.* **2001**, *202*, 2926–2946.
(3) Krause, S.; Zander, F.; Bergmann, G.; Brandt, H.; Wertmer, H.; Finkelmann, H. *C. R. Chimie* **2009**, *12*, 85–104.
(4) Hiraoka, K.; Kobayasi, M.; Kazama, R.; Finkelmann, H. *Macromolecules* **2009**, *42*, 5600–5604.
(5) Corbett, D.; Warner, M. *Sens. Actuators A* **2009**, *149*, 120–129.
(6) Corbett, D.; Warner, M. *Soft Matter* **2009**, *5*, 1433–1439.
(7) Li, J.; Tammer, M.; Kremer, F.; Komp, A.; Finkelmann, H. *Eur. Phys. J. E* **2005**, *17*, 423–428.
(8) Bahr, C. In *Chirality in Liquid Crystals*; Kitzerow, H., Bahr, C., Eds.; Springer-Verlag: New York, 2001.
(9) Hird, M.; Goodby, J. W.; Hindmarsh, P.; Lewis, R. A.; Toyne, K. J. *Ferroelectrics* **2002**, *276*, 219–237.
(10) Brand, H. R. *Makromol. Chem., Rapid Commun.* **1989**, *10*, 441–445.
(11) Lagerwall, J. P. F.; Giesselmann, F. *ChemPhysChem* **2006**, *7*, 20–45.
(12) Lehmann, W.; Hartmann, L.; Kremer, F.; Stein, P.; Finkelmann, H.; Kruth, H.; Diele, S. *J. Appl. Phys.* **1999**, *86*, 1647–1652.
(13) Spillmann, C. M.; Ratna, B. R.; Naciri, J. *Appl. Phys. Lett.* **2007**, *90*, 021911.
(14) Walba, D. M.; Yang, H.; Shoemaker, R. K.; Keller, P.; Shao, R.; Coleman, D. A.; Jones, C. D.; Nakata, M.; Clark, N. A. *Chem. Mater.* **2006**, *18*, 4576–4584.
(15) Jákli, A.; Éber, N.; Bata, L. *Polym. Adv. Technol.* **1992**, *3*, 269–274.
(16) Vallerien, S. U.; Kremer, F.; Fischer, E. W.; Kapitza, H.; Zentel, R.; Poths, H. *Makromol. Chem., Rapid Commun.* **1990**, *11*, 593–598.
(17) Kremer, F.; Lehmann, W.; Skupin, H.; Hartmann, L.; Stein, P.; Finkelmann, H. *Polym. Adv. Technol.* **1998**, *9*, 672–676.
(18) Lehmann, W.; Gattinger, P.; Keck, M.; Kremer, F.; Stein, P.; Eckert, T.; Finkelmann, H. *Ferroelectrics* **1998**, *208*, 373–383.
(19) Brehmer, M.; Zentel, R.; Giesselmann, F.; Germer, R.; Zugenmaier, P. *Liq. Cryst.* **1996**, *21*, 589–596.
(20) Meier, W.; Finkelmann, H. *Makromol. Chem., Rapid Commun.* **1990**, *11*, 599–605.
(21) Lehmann, W.; Skupin, H.; Tolksdorf, C.; Gebhard, E.; Zentel, R.; Krüger, P.; Lösche, M.; Kremer, F. *Nature* **2001**, *410*, 447–450.
(22) Stein, P.; Finkelmann, H. In *Chirality in Liquid Crystals*; Kitzerow, H., Bahr, C., Eds.; Springer-Verlag: New York, 2001.
(23) Hiraoka, K.; Uematsu, Y.; Stein, P.; Finkelmann, H. *Macromol. Chem. Phys.* **2002**, *203*, 2205–2210.
(24) Zentel, R.; Reckert, G.; Bualek, S.; Kapitza, H. *Makromol. Chem.* **1989**, *190*, 2869–2884.
(25) Adams, J. M.; Warner, M. *Phys. Rev. E* **2008**, *77*, 021702.
(26) Komp, A.; Finkelmann, H. *Macromol. Rapid Commun.* **2007**, *28*, 55–62.
(27) Komp, A.; Rühe, J.; Finkelmann, H. *Macromol. Rapid Commun.* **2005**, *26*, 813–818.
(28) Sanchez-Ferrer, A.; Finkelmann, H. *Macromolecules* **2008**, *41*, 970–980.
(29) Hiraoka, K.; Finkelmann, H. *Macromol. Rapid Commun.* **2001**, *22*, 456–460.
(30) Heinze, P.; Finkelmann, H. *Macromolecules* **2010**, DOI: 10.1021/ma1002084.
(31) Eckert, T.; Finkelmann, H.; Keck, M.; Lehmann, W.; Kremer, F. *Macromol. Rapid Commun.* **1996**, *17*, 767–773.
(32) Brehmer, M.; Zentel, R.; Wagenblast, G.; Siemensmeyer, K. *Macromol. Chem. Phys.* **1994**, *195*, 1891–1904.
(33) Das-Gupta, D. *An Introduction to Molecular Electronics*; Petty, M. C., Bryce, M. R., Bloor, D., Eds.; Oxford University Press: New York, 1995.
(34) Hiraoka, K.; Stein, P.; Finkelmann, H. *Macromol. Chem. Phys.* **2004**, *205*, 48–54.